Nat. Hazards Earth Syst. Sci. Discuss., 3, 675–695, 2015
www.nat-hazards-earth-syst-sci-discuss.net/3/675/2015/
doi:10.5194/nhessd-3-675-2015

Natural Hazards and Earth System Sciences
Open Access
Discussions

Formation time and mean movement velocities of the 7 August Zhouqu debris flows extracted from broadband seismic records

Z. Li[1], X. Huang[1], Q. Xu[2], J. Fan[1], D. Yu[1], Z. Hao[3], and X. Qiao[4]

[1]China Earthquake Networks Center, Beijing, 100045, China
[2]State Key Laboratory of Geohazard Prevention and Geoenvironment Protection, Chengdu University of Technology, Chengdu, 610059, China
[3]Lanzhou Institute of Seismology, China Earthquake Administration, Lanzhou, 730000, China
[4]Institute of Seismology, China Earthquake Administration, Wuhan, 430071, China

Received: 15 December 2014 – Accepted: 31 December 2014 – Published: 22 January 2015

Correspondence to: X. Huang (huangxh19850216@gmail.com)

Published by Copernicus Publications on behalf of the European Geosciences Union.

Abstract

The catastrophic Zhouqu debris flows, which were induced by heavy rainfall, occurred at approximately midnight of 7 August 2010 (Beijing time, UTC + 8) and claimed 1765 lives. Broadband seismic signals recorded by the Zhouqu seismic station nearby are acquired and analyzed in this paper. The seismic signals are divided into two separate parts for the first time using the crucial time of 23:33:10 (Bejing time, UTC +8), with distinctly different frequency characteristics on time-by-time normalized spectrograms and amplitude increasing patterns on smoothed envelopes. They are considered to be generated by the development stage and the maturity stage of the Sanyanyu debris flow respectively. Seismic signals corresponding to the development stage have a broader main frequency band of approximately 0–15 Hz than that of the maturity stage, which is around 1–10 Hz. The N–S component can detect the development stage of the debris flow about 3 min earlier than other components due to its southward flow direction. Two sub-stages within the maturity stage are recognized from best-fitted amplitude increasing velocities and the satellite image of the Sanyanyu flow path and the mean movement velocities of the Sanyanyu debris flow during these two sub-stages are estimated to be 9.2 and 9.7 $m\,s^{-1}$ respectively.

1 Introduction

Zhouqu County is located in Longnan Prefecture and belongs to Gansu Province in the northwestern part of China. It is geologically part of the conjunction area of tectonic blocks in the E–W direction and in the middle of the N–S seismotectonic zone. This area, which is largely influenced by tectonisms that result from the western Tibetan Plateau, suffers from high tectonic activities and destructive earthquakes frequently. As a consequence, fold belts and faults are widely distributed; and loose geological structures and materials can be easily detected everywhere. Geological hazards, such as rock collapses and debris flows have been big threats to local residents

NHESSD
3, 675–695, 2015

ever since ancient times. The topography in this area varies dramatically due to fold belts and faults, and the maximum altitude difference is up to 2488 m. Most of its gullies have steep slopes, more than half of which are steeper than 25°. Sufficient available loose materials, unstable geological structures and steep slopes on the catchment are the necessary conditions for giant debris flows occurring in this area (Takahashi, 1981).

At approximately midnight of 7 August 2010 (Beijing time, UTC + 8), two giant debris flows induced by heavy rainfall hit Zhouqu city and claimed 1765 lives (Tang et al., 2011; Wang et al., 2013b; Yu et al., 2010). A total volume of 2.2 million m^3 was transported and deposited on an existing debris fan. The heads of debris flows rushed into the Bailongjiang River and formed a 3 km long barrier lake (Fang et al., 2010). Water ran into Zhouqu city and caused further damages after being stopped by the newly formed dam (Yu et al., 2010). Most previous studies about these debris flows mainly focused on the geological and precipitation perspectives (Liu et al., 2011; Zhang et al., 2012; Wang et al., 2013a). However, at least three questions are still left unresolved: first, we only know the time that the debris flows rushed into the Zhouqu city, but what is their formation time? Second, what kind of frequency characteristics do seismic signals have for the development stage and the maturity stage of the debris flows? Are there any differences? Third, could mean movement velocities of debris flows be estimated for different stages? The questions above are what we attempt to resolve in this paper.

Digital broadband seismic observation networks have been gradually established and completed in China. These networks can help to acquire new information and explain new phenomena in seismic observations. Broadband seismic signals have also been widely used in geological hazard researches, such as landslides (Brodsky et al., 2003; Chen et al., 2013; Feng, 2011; Kao et al., 2012; Lin et al., 2010; Yamada et al., 2012) rockfalls (De Angelis et al., 2007; Norris, 1994; Vilajosana et al., 2008) avalanches, debris flows (Arattano, 1999; Burtin et al., 2009) and other block movements (Deparis et al., 2008; Suriñach et al., 2005). These studies are receiving growing attentions. Recent studies show that the quantitative extraction and analysis of seismic networks data can explain the key processes, as well as landslide and debris

NHESSD
3, 675–695, 2015

flow mechanisms, especially their geological characteristics (Chen et al., 2013; Petley, 2013; Ekström and Stark, 2013). In the present study, broadband seismic records are used to research the giant Zhouqu debris flows occurred in 7 August 2010. The formation time of Sanyanyu debris flow is revealed to be 23:33:10 (Bejing time, UTC +8) for the first time. Combined with the satellite image of the Sanyanyu flow path, the mean movement velocities of Sanyanyu debris flow during two sub-stages are estimated to be 9.2 and 9.7 $m\,s^{-1}$ respectively. This study validates that broadband seismic signals recorded by seismic stations deployed at proper positions can be used to extract key parameters of debris flows, such as formation time and mean movement velocity.

2 Seismic data

The giant 7 August Zhouqu debris flows occurred in the catchments of the Sanyanyu and Luojiayu torrents. A total volume of 2.2 million m^3 was transported and deposited on an existing debris fan and into a river, and about 64 % of them originated from the Sanyanyu drainage area (Tang et al., 2011). Compared with Luojiayu debris flow, the Sanyanyu debris flow has a longer path and a larger drainage area (Tang et al., 2011). The Zhouqu seismic station is located downstream of Sanyanyu gully and positioned only 150 m away from the exit (Fig. 1). Thus, seismic records mainly represent energy released in Sanyanyu gully. The longitude, latitude, and altitude of the station are 104.4° E, 33.8° N, and 1460 m respectively. The bedrock where the seismometer is deployed is limestone, which guarantees the high quality of seismic records used in this research. The giant Sanyanyu debris flow hit the Zhouqu seismic station and destroyed its power system at approximately 23:40 LT according to monitoring logs. This time can also be confirmed by the end time of seismic records. The debris flow then rushed into Zhouqu city only approximately 2.1 min later (Liu et al., 2011), killed many people and caused large economic losses. The seismic signals recorded by a CMG-3ESPC broadband seismic seismometer with the sample rate of 100 Hz exhibited continuous variations in time and frequency domains tens of minutes before the records ended.

NHESSD
3, 675–695, 2015

The amplitude of seismic signals increases in approximately an exponential way with time, which is partly because the actual increase of the debris flow's kinematic energy and partly because the approaching of the debris flow with time; and the maximum amplitude at the end of the signal is approximately 200 times larger than that of the background signals. Seismic signals about 15 min before the end of records (i.e. from 23:25 LT) are selected to reveal intrinsic processes of this debris flow, and their waveforms are shown in Fig. 2.

3 Methodology and results

3.1 Development stage and maturity stage of the giant Sanyanyu debris flow

Signal characteristics are acquired and analyzed in time-frequency domain in the first place. Time-frequency analysis is very effective in analyzing non-stationary signals and widely used in signals processes. Short-time Fourier Transform, wavelet transform and S-transform are among the most frequently used methods. In this study, short-time Fourier transform is applied to the selected seismic signals with a moving time window of 10.24 s. Spectrogram has the advantage of showing global energy variation patterns temporally and spatially in the same image. But, when dealing with peculiar signals with imbalanced energy distribution in time domain as in this case, the frequency distribution could be misleading. Figure 2 reveals that the amplitude of selected seismic signals increases in approximately an exponential way with time. In spectrograms of this kind of signals, energy distributions for different frequency components in low amplitude regions are usually shadowed by that of high amplitude regions, which implies that the main frequency band cannot be correctly observed for low amplitude regions. Given that we are more interested in the energy distributions than the total energy, amplitude influences are eliminated for spectrograms by normalizing each time component to 0–1. They are called time-by-time normalized spectrograms and shown in Fig. 3. The envelopes of selected seismic signals are also acquired using Hilbert Transform and

NHESSD
3, 675–695, 2015

shown in Fig. 3 after being smoothed using the time window of 10.24 s, the same as that used in spectrogram calculations.

Generally speaking, background signals are mainly composed of linear drifting and low-frequency oscillations with periods of several seconds, their peak frequency is no more than 0.5 Hz. Signals with a broader main frequency band as large as 0 to 10 Hz and beyond are most probably generated by the debris flows and related events. The most obvious feature of spectrograms in Fig. 3 is that they can be divided into two separate parts with distinctly different frequency distribution characteristics using the time of 23:33:10. For the left part, the effective signals are widely distributed with the main frequency band of as broad as 0 Hz to approximately 15 Hz. The horizontal components (i.e. E–W component and N–S component) contain more effective signals than the vertical component (i.e. U-D component). The energy distribution in the frequency domain for the right part is relatively regular. The main frequency band of the U-D component shifts from approximately 1.5–8.6 Hz at the separation time to 3.5-10.6 Hz at the end of the signal in a near-linear manner without any expansion. As for the horizontal components, main frequency band changed from 1.8–7.1 Hz to 2.8–9.3 Hz for the E–W component and from 2.3–7.2 Hz to 3.3–11.2 Hz for the N–S component, probably due to the Doppler Effect. The Doppler Effect affects the horizontal components much stronger than the vertical component because the Sanyanyu debris flow is mainly in the horizontal direction.

Figure 3 also reveals that the smoothed envelopes of seismic signals are more than 10 times larger than that of background signals at the time of 23:33:10 and rapidly increase afterward in an unprecedented velocity. Based on the spectrograms and smoothed envelopes, we claim that seismic signals generated by the giant Sanyanyu debris flow can be divided into two separate parts with distinctly different frequency characteristics corresponding to the development stage and maturity stage of the debris flow respectively. Unlike earthquakes and landslides, debris flows do not break out suddenly. It takes some time to accumulate water and loose materials before a large and destructive energy release is fully formed. Seismic signals generated by these two

NHESSD
3, 675–695, 2015

stages before and after the formation of a debris flow are quite different, especially in the frequency domain. We define the crucial time of 23:33:10 as the formation time (FT) of the giant Sanyanyu debris flow, after which the debris flow reached its maturity.

It is almost impossible to determine when a debris flow starts developing. Even from the first stream of water running, the first pile of loose materials moving and the first boulder falling, the development stage of a debris flow starts. As loose materials gathering and their kinematic energy gradually increasing, seismic signals generated by them become detectable by seismometers. However, a rough start time can be revealed under a given criterion. Here, the short-term average/long-term average (STA/LTA) approach (Chen et al., 2013; Kao et al., 2012) is employed to determine the start time (ST) of the development stage of the Sanyanyu debris flow. Threshold and time window of 1.6 and 15 s, respectively, are adopted in the present study and the procedure is described as follows. First, the mean absolute values of background signals are calculated for each component. And then we move a time window with the given width step by step to calculate mean absolute values inside. If a calculated value exceeds the threshold, we assign the start time. Results of three components are 23:30:16.48 (U–D), 23:30:12.56 (E–W), and 23:27:19.48 (N–S) respectively. It can be observed that the ST of the N–S component is approximately 3 min earlier than that of other components. Spectrograms also reveal that the horizontal components (E–W and N–S) can detect effective signals much earlier than the vertical component (U-D); and within horizontal components, the N–S component is earlier than the E–W component. Given that debris flows mainly move in the horizontal direction, the energy amplification is much faster for the horizontal direction than the vertical direction and can be detected sooner by horizontal components (E–W and N–S). The direction of the main debris flow path in this study is mainly north–south (Fig. 1). Therefore, the calculated ST of the N–S direction is much earlier than that of the E–W and U-D components.

NHESSD
3, 675–695, 2015

3.2 Estimation of the Sanyanyu debris flow movement velocities

To reveal the amplitude variation patterns of seismic signals with time, firstly the Hilbert Transform is adopted to get the envelopes of signals; and subsequently, the envelopes are linearly best-fitted to get the mean amplitude increasing velocities using a moving time window of 1 min. To eliminate influences from source approaching with time, we multiply the results by the function scale(t), which is defined as:

$$\text{scale}(t) = e^{-t/120}$$

Where t is time in second and starts from 23:30. The scaled best-fitted amplitude increasing velocities for three components and scale function are shown in Fig. 4.

Amplitude of seismic signals can roughly represent the kinematic energy released by the debris flow. Figure 4 shows that there are at least four magnificent peaks in the maturity stage corresponding to a sequence of fast energy accumulation stages of the debris flow, which could be caused by the increase of movement velocity and/or materials. These two manners have different characteristics in amplitude increase patterns. Material increase caused energy increase corresponds to the synchronous increase of amplitude for the three components; while movement velocity increase caused energy increase corresponds to more significant increase in the component of the movement direction than other components. Four key time points (i.e. KT1, KT2, KT3 and KT4) are depicted in Fig. 4 to help carrying out the following discussions. Satellite image of the Sanyanyu flow path snapshotted from Google Earth is shown in Fig. 5 to analyze different spatial stages of the giant Sanyanyu debris flow. The Sanyanyu flow path is depicted using color solid lines and the altitude profile along the path is given sideward as well. A colluvial deposit area described as a significant energy accumulation region (Tang et al., 2011) is also sketched in Fig. 5 using a gray solid line.

Because the Sanyanyu debris flow moved mainly in the horizontal direction, the amplitude increase of the U-D component is mostly from the material increase instead of the movement velocity increase. This can explain that the scaled best-fitted amplitude increasing velocities of the horizontal components are larger than that of the

NHESSD
3, 675–695, 2015

vertical component almost in the whole maturity stage; and that the Doppler Effect affects the horizontal components much stronger. As for the horizontal components, the amplitude increase could be from the increase of materials and movement velocities. In the first case, the scaled best-fitted amplitude increasing velocities of horizontal components vary with that of the vertical component. In the second case, the amplitude of the component in the acceleration direction increase faster than other components. Figure 4 reveals that from KT2 to KT3, the amplitude of the N–S component increases much faster than that of the E–W and U-D components; from KT3 to KT4, the amplitude of the E–W component increases rapidly. This phenomenon corresponds to a path shape of southward/northward in the beginning and turn to eastward/westward in the end, which is in consistent with the path section depicted using orange solid line in Fig. 5. This path section is southward in the beginning and then turns to eastward in the end. Therefore, we believe that seismic signals between K2 and K4 were generated when the Sanyanyu debris flow moved on this path section. Before KT2 in Fig. 4, there is a significant peak section with an approximately synchronous increase pattern for three components. Meanwhile, the path section before the orange solid line in Fig. 5 is within the colluvial deposit area. When the Sanyanyu debris flow moved on this path section, seismic signals with amplitude increase patterns between KT1 and KT2 could be generated. Based on the above information, the seismic signals corresponding to the maturity stage is further divided into four sub-stages, with the first one from FT to KT1, the second one from KT1 to KT2, the third one from KT2 to KT4, and the last one from KT4 to the end. Four corresponding spatial stages are depicted in Fig. 5 using blue, yellow, orange and red solid lines respectively. The time intervals and length of path sections for different stages are listed in Table 1. The mean movement velocities of the Sanyanyu debris flow during stage 2 and 3 are estimated to be 9.2 and 9.7 $\mathrm{m\,s^{-1}}$ respectively.

NHESSD
3, 675–695, 2015

4 Discussions

It is necessary to discriminate effective signals from background signals before further processes. Normally, this can be achieved by recognizing different amplitude characteristics in time domain and energy distribution characteristics in frequency domain. Amplitude differences between effective signals and background signals in time domain can be easily recognized; but for the frequency domain it is not that obvious. Spectrograms are frequently used to characterize frequency distributions along time; but they contain not only frequency information but also amplitude information in a global way. They are merged together. When the amplitude is imbalanced globally, signals that contain effective information in frequency domain but with relatively low amplitude are covered up like the situation in this case. Time-by-time normalized spectrogram is used in signal processing for the first time and proves a good tool. It normalizes each time component of a spectrogram to eliminate influences from the imbalanced amplitude distribution and can reveal true frequency distributions. By using this method, development stage and maturity stage of the giant Sanyanyu debris flow are distinctly separated for the first time. This method may also be used to detect effective information of other kinds of event such as landslides, earthquakes and volcano eruptions.

The development of a debris flow starts from collecting loose materials and water. But, from the development stage to the maturity stage of a debris flow, it is not a simply quantitative change; instead, a qualitative change happens. Before and after the formation time, the differences of seismic signals in amplitude and frequency are quite clear. The main frequency band of seismic signals corresponding to the development stage is broader than that of the maturity stage. Yet, the seismic signals corresponding to the maturity stage is more regular. The component in the direction of a debris flow movement can detect the development of the debris flow earlier, which can be used in alert systems. The main frequency band of seismic signals corresponding to the maturity stage of the Sanyanyu debris flow expanded 0, 22.64 and 61.22 % for U-D,

NHESSD
3, 675–695, 2015

E–W and N–S components respectively, which implies that the Doppler Effect affects seismic signals in the component of the movement direction the strongest.

Mean movement velocities of the Sanyanyu debris flow during sub-stages 2 and 3 are estimated to be 9.2 and 9.7 $m\,s^{-1}$ respectively. These results are in consistence with the previous estimation (Tang et al., 2011). The estimation result that the mean movement velocity of the debris flow in sub-stage 3 is larger than that in sub-stage 2 is consistence with our previous judgment that a significant portion of the energy increase in the sub-stage 3 is from the movement velocity increase. As for the sub-stages 1 and 4, the exact formation location of the Sanyanyu debris flow is very hard to determine from the satellite image. Also, the Sanyanyu debris flow lasted several minutes. When the head of the debris flow destroyed the power system of the Zhouqu seismic station, the seismic source was not necessarily reached the station. Therefore, the mean movement velocities in these two sub-stages are left unresolved. The length of the time window used in calculation of the best-fitting amplitude increasing velocity is 60 s. Given the movement velocity of the debris flow of approximately 10 $m\,s^{-1}$, the spatial resolution is about 600 m. Sub-stages have a smaller spatial scale cannot be rightly resolved using this data.

5 Conclusions

The 7 August Zhouqu debris flows, which were induced by very heavy rainfall killed 1765 people and caused great economic losses. Zhouqu seismic station located on the path to Zhouqu city was destroyed by the debris flows at approximately 23:40 LT on the same date, which marks the time when the head of the debris flows reached the station. The seismic signals recorded by the Zhouqu seismic station before being destroyed are analyzed in this paper. The signals are divided into two separate parts for the first time using the crucial time of 23:33:10, with distinctly different frequency characteristics on time-by-time normalized spectrograms and amplitude increasing patterns on smoothed envelopes. They are considered to be generated by the development

NHESSD
3, 675–695, 2015

stage and the maturity stage of the Sanyanyu debris flow respectively. Seismic signals corresponding to the development stage have a broader main frequency band of approximately 0–15 Hz than that of the maturity stage, which is around 1–10 Hz. The main frequency band shifted to the high frequency direction with the seismic source approaching for all of the three components; and it also expanded 22.64 and 61.22 % for E–W and N–S components due to the Doppler Effect. The N–S component can detect the development stage of the debris flow about 3 min earlier than other components due to its southward flow direction. The seismic signals corresponding to the maturity stage is further divided into four sub-stages according to peaks from scaled best-fitted amplitude increasing velocities. Combined with the satellite image of the Sanyanyu flow path, the mean movement velocities of the Sanyanyu debris flow in sub-stages 2 and 3 are estimated to be about 9.2 and 9.7 $m\,s^{-1}$ respectively. Our results show that broadband seismic signals recorded by seismic stations deployed at proper positions can be used to extract key parameters of debris flows and research their formation mechanisms.

Author contributions. Z. Li, X. Huang and Q. Xu discussed and determined the overall framework of this study; J. Fan, D. Yu, Z. Hao and X. Qiao prepared the seismic data and did field investigations; X. Huang analyzed the seismic data and prepared the manuscript with contributions from all co-authors.

Acknowledgements. We would like to thank Liu Ruifeng, Huang Zhibin, and Zhao Yong from the China Earthquake Networks Center for their helpful comments on seismic wave recognition. We also thank Zeng Wenhao and Niu Yanping from the Lanzhou Institute of Seismology for their kind help in the field investigation. Liu Zhumei from the Institute of Seismology also helped us in preparing Fig. 1. Satellite image of Sanyanyu flow path in Fig. 5 is snapshotted form Google Earth. This research is financially supported by the 973 Program 2013CB733200 and 863 Program 2012AA121302.

NHESSD
3, 675–695, 2015

References

Arattano, M.: On the use of seismic detectors as monitoring and warning systems for debris flows, Nat. Hazards, 20, 197–213, 1999.

Brodsky, E. E., Gordeev, E., and Kanamori, H.: Landslide basal friction as measured by seismic waves, Geophys. Res. Lett., 30, 2236, doi:10.1029/2003GL018485, 2003.

Burtin, A., Bollinger, L., Cattin, R., Vergne, J., and Nábělek, J. L.: Spatiotemporal sequence of Himalayan debris flow from analysis of high-frequency seismic noise, J. Geophys. Res.-Earth, 114, F04009, doi:10.1029/2008JF001198, 2009.

Chen, C.-H., Chao, W.-A., Wu, Y.-M., Zhao, L., Chen, Y.-G., Ho, W.-Y., Lin, T.-L., Kuo, K.-H., and Chang, J.-M.: A seismological study of landquakes using a real-time broad-band seismic network, Geophys. J. Int., 194, 885–898, 2013.

De Angelis, S., Bass, V., Hards, V., and Ryan, G.: Seismic characterization of pyroclastic flow activity at Soufrière Hills Volcano, Montserrat, 8 January 2007, Nat. Hazards Earth Syst. Sci., 7, 467–472, doi:10.5194/nhess-7-467-2007, 2007.

Deparis, J., Jongmans, D., Cotton, F., Baillet, L., Thouvenot, F., and Hantz, D.: Analysis of rock-fall and rock-fall avalanche seismograms in the French Alps, B. Seismol. Soc. Am., 98, 1781–1796, 2008.

Ekström, G. and Stark, C. P.: Simple scaling of catastrophic landslide dynamics, Science, 339, 1416–1419, 2013.

Fang, H. Y., Cai, Q. G., Li, Q. Y., Sun, L. Y., and He, J. J.: Causes and countermeasures of giant flash flood and debris flow disaster in Zhouqu County in Gansu Province on 7 August 2010, Science of Soil and Water Conservation, 8, 14–18, 2010 (in Chinese).

Feng, Z.: The seismic signatures of the 2009 Shiaolin landslide in Taiwan, Nat. Hazards Earth Syst. Sci., 11, 1559–1569, doi:10.5194/nhess-11-1559-2011, 2011.

Kao, H., Kan, C.-W., Chen, R.-Y., Chang, C.-H., Rosenberger, A., Shin, T.-C., Leu, P.-L., Kuo, K.-W., and Liang, W.-T.: Locating, monitoring, and characterizing typhoon-linduced landslides with real-time seismic signals, Landslides, 9, 557–563, 2012.

Lin, C. H., Kumagai, H., Ando, M., and Shin, T. C.: Detection of landslides and submarine slumps using broadband seismic networks, Geophys. Res. Lett., 37, L22309, doi:10.1029/2010GL044685, 2010.

NHESSD
3, 675–695, 2015

Liu, C. Z., Miao, T. B., Chen, H. Q., Dong, K. J., Li, Z. H., and Li, H. J.: Basic feature and origin of the "8 × 8" mountain torrent-debris flow disaster happened in Zhouqu County, Gansu, China, Aug. 8, 2010, Geological Bulletin of China, 30, 141–150, 2011 (in Chinese).

Norris, R. D.: Seismicity of rockfalls and avalanches at three Cascade Range volcanoes: implications for seismic detection of hazardous mass movements, B. Seismol. Soc. Am., 84, 1925–1939, 1994.

Petley, D. N.: Characterizing giant landslides, Science, 339, 1395–1396, 2013.

Suriñach, E., Vilajosana, I., Khazaradze, G., Biescas, B., Furdada, G., and Vilaplana, J. M.: Seismic detection and characterization of landslides and other mass movements, Nat. Hazards Earth Syst. Sci., 5, 791–798, doi:10.5194/nhess-5-791-2005, 2005.

Takahashi, T.: Estimation of potential debris flows and their hazardous zones: soft countermeasures for a disaster, Journal of Natural Disaster Science, 3, 57–89, 1981.

Tang, C., Rengers, N., van Asch, Th. W. J., Yang, Y. H., and Wang, G. F.: Triggering conditions and depositional characteristics of a disastrous debris flow event in Zhouqu city, Gansu Province, northwestern China, Nat. Hazards Earth Syst. Sci., 11, 2903–2912, doi:10.5194/nhess-11-2903-2011, 2011.

Vilajosana, I., Suriñach, E., Abellán, A., Khazaradze, G., Garcia, D., and Llosa, J.: Rockfall induced seismic signals: case study in Montserrat, Catalonia, Nat. Hazards Earth Syst. Sci., 8, 805–812, doi:10.5194/nhess-8-805-2008, 2008.

Wang, G. L., Zhang, M. S., Yu, G. Q., and Ye, W. J.: Factor analysis for catastrophic debris flows on August 8, 2010 in Zhouqu City of Gansu, China, J. Mt. Sci., 31, 349–355, 2013a (in Chinese).

Wang, L. M., Wu, Z. J., Wang, P., and Chen, T.: Characteristics, causation, and rehabilitation of Zhouqu extraordinarily serious debris flows in 2010, China, J. Cent South Univ. T., 20, 2342–2348, 2013b.

Yamada, M., Matsushi, Y., Chigira, M., and Mori, J.: Seismic recordings of landslides caused by typhoon Talas (2011), Japan, Geophys. Res. Lett., 39, L13301, doi:10.1029/2012GL052174, 2012.

Yu, B., Yang, Y. H., Su, Y. C., Huang, W. J., and Wang, G. F.: Research on the giant debris flow hazards in Zhouqu County, Gansu Province on August 7, 2010, J. Eng. Geol., 18, 437–444, 2010 (in Chinese).

NHESSD
3, 675–695, 2015

Zhang, Z. X., Zhang, Q., Tao, J. C., Sun, Y., and Zhao, Q. Y.: Climatic and geological environmental characteristics of the exceptional debris flow outburst in Zhouqu, Gansu Province, on 8 August, 2010, J. Glaciol. Geocryol., 34, 898–905, 2012 (in Chinese).

NHESSD
3, 675–695, 2015

Table 1. Time intervals of sub-stages 1–4 and distances of sub-stages 2 and 3. Mean movement velocities of the Sanyanyu debris flow in sub-stages 2 and 3 are also provided.

Sub-stage	1	2	3	4
Time interval (s)	128.78	108.47	91.75	36.54
Distance (m)	–	999.57	892.03	–
Mean velocity ($m s^{-1}$)	–	9.2	9.7	–

NHESSD
3, 675–695, 2015

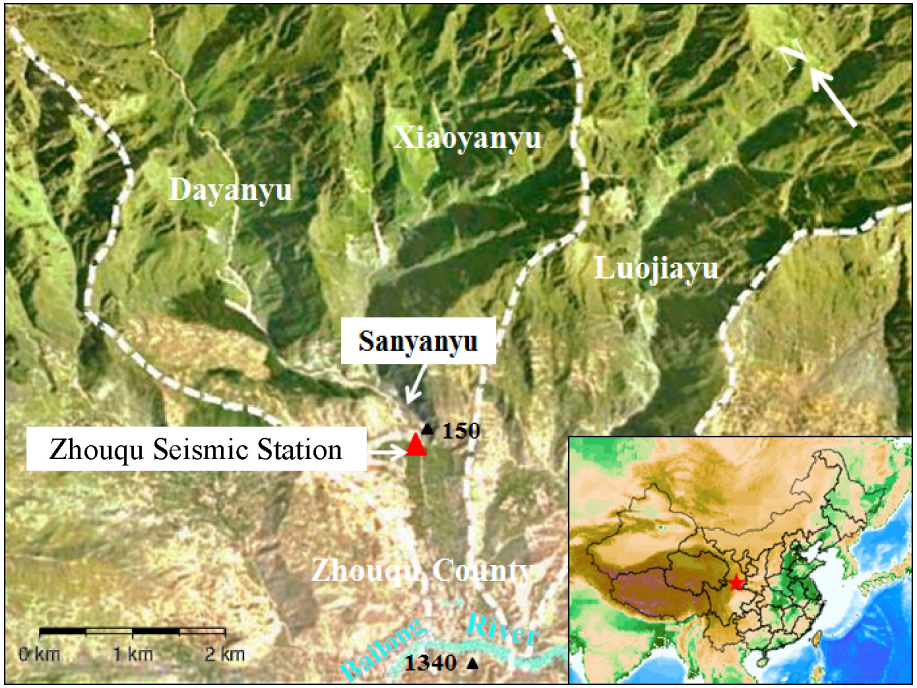

Figure 1. Locations of the Zhouqu seismic station (red solid triangle), Sanyanyu Gully, and Luojiayu Gully.

NHESSD
3, 675–695, 2015

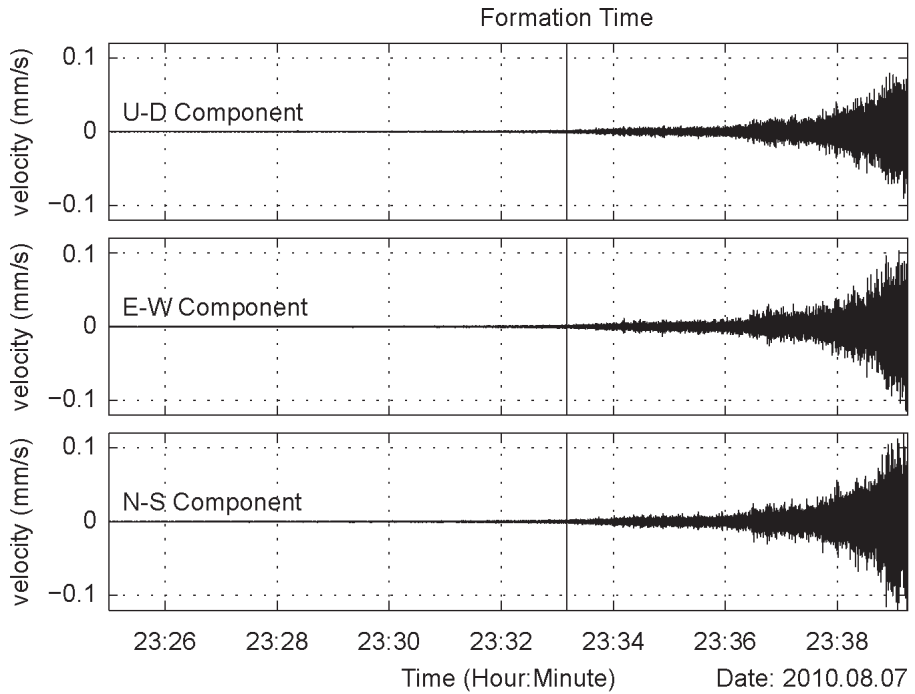

Figure 2. Seismic waveforms of three components. The top to bottom images are U–D, E–W, and N–S components respectively. The formation time is marked by using black solid lines.

NHESSD
3, 675–695, 2015

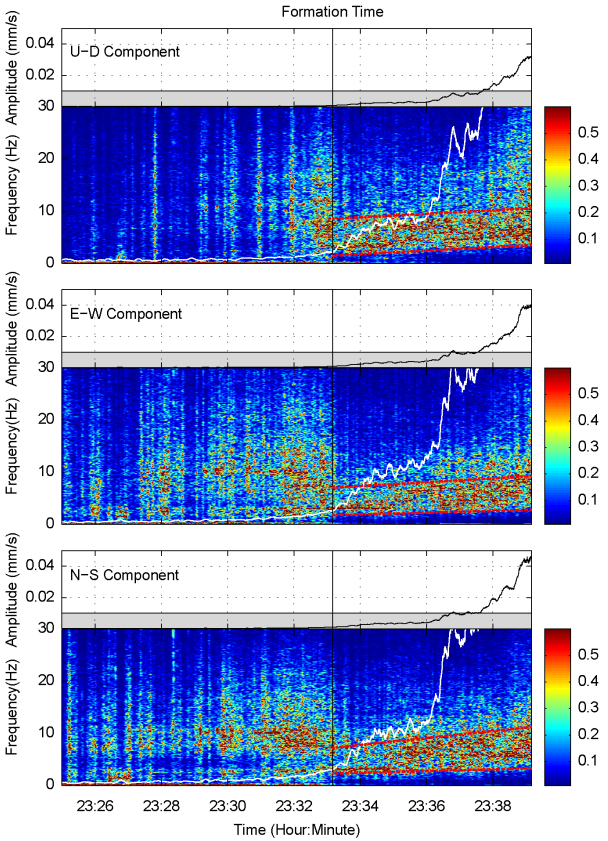

Figure 3. Smoothed envelopes (upper panel) and time-by-time normalized spectrograms (lower panel) of three components. The formation time is marked by using black solid lines. The smoothed envelopes in the shadow regions are enlarged and superimposed on the spectrograms using white solid lines. The main frequency bands of the three components are roughly depicted between the red dashed lines.

NHESSD
3, 675–695, 2015

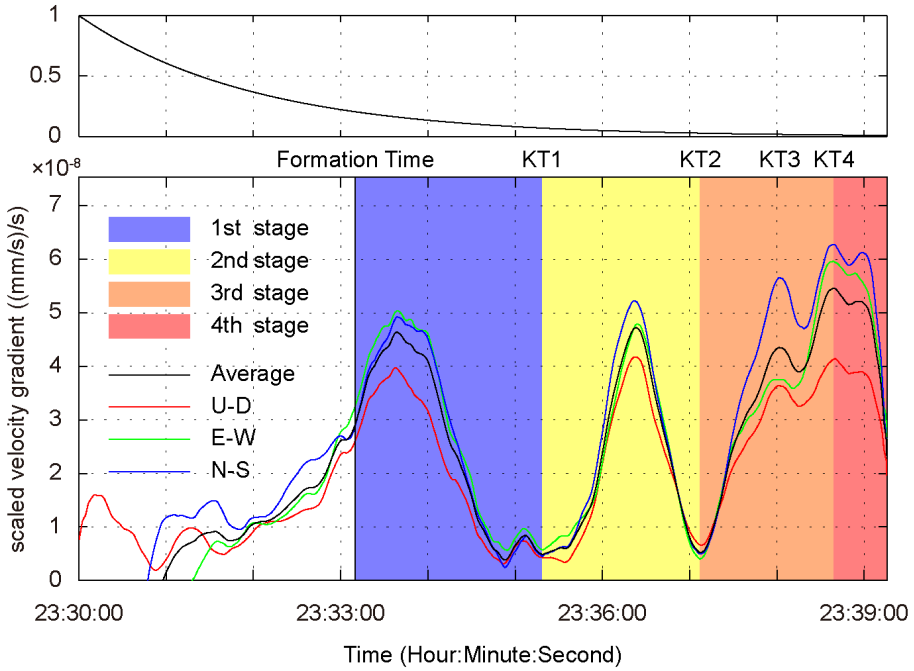

Figure 4. Scale function (upper panel) and scaled best-fitted amplitude increasing velocities (lower panel). The formation time and key time points (KT1, KT2, KT3 and KT4) are also depicted. The maturity stage is further divided into 4 sub-stages and distinguished using different background colors.

NHESSD
3, 675–695, 2015

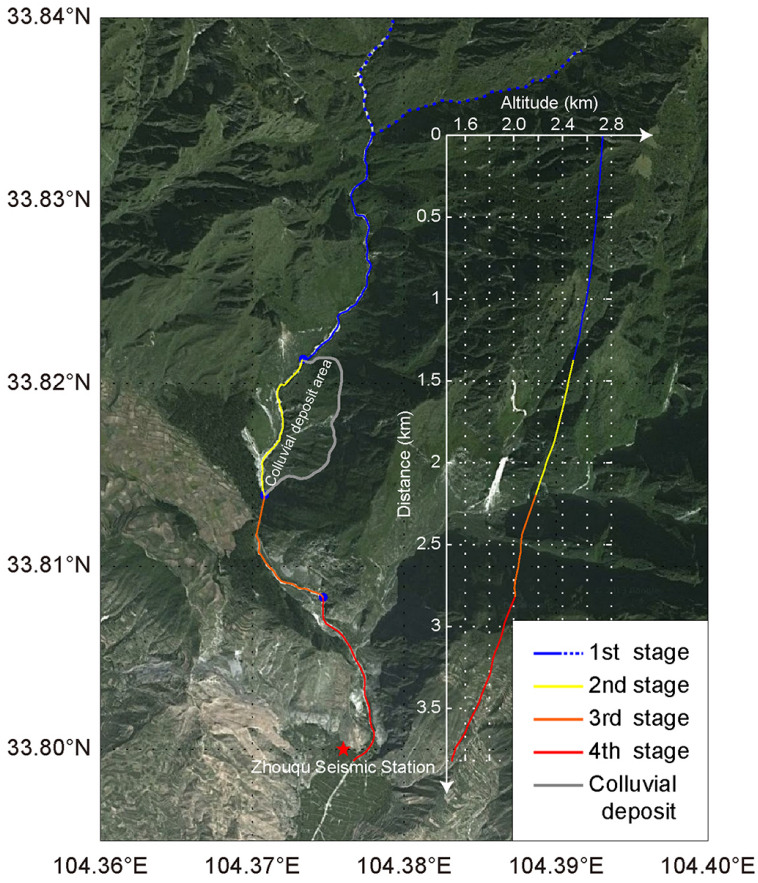

Figure 5. Satellite image of the Sanyanyu flow path, depicted using color solid lines with different colors corresponding to different sub-stages. The altitude profile is provided sideward. A significant colluvial deposit area is also sketched using a gray solid line.

NHESSD
3, 675–695, 2015